Fault diagnosis using robust cascade observers with application to spacecraft attitude control

WANG Yu-lei, MA Guang-fu, LI Chuan-jiang

王宇雷, 马广富, 李传江

(Dept. of Control Science and Engineering, Harbin Institute of Technology, Harbin 150001, China, hit_raynking@yahoo.cn)

Abstract: This paper proposes a new gyro and star sensor fault diagnosis architecture that designs two groups of cascade H_∞ optimal fault observers using LMI for spacecraft attitude control systems. The basic idea of the approach is to identify the gyro fault to good effect first and then makes a further diagnosis for the star sensor based on the former. The H_∞ optimal fault observer in design has the robustness with respect to model uncertainties and diagnosis uncertainties. Its robustness to unknown inputs is as a special study in frequency domain. Finally, simulation results demonstrate the effectiveness and feasibility of the proposed control algorithm.

Key words: spacecraft attitude control system; fault diagnosis; H_∞ optimal fault observer; cascade observer

CLC number: TP273 **Document code**: A **Article ID**: 1005-9113(2011)04-0123-09

Autonomy and fail-recovery operation in spacecraft design on-board is critical issue in the presence of faults and failures in sensors, actuators, and other components. Comparing with the ground systems, it is not practical to have physical backup systems based on such as triple module redundancy with voting[1] and quadruple redundancy with parity check[2] in spacecraft systems. This is due to the relational increase in cost and also space limitation on-board the spacecraft. Consequently, analytical redundancy is utilized as a powerful method to compare the expected behavior of the system with the observed behavior.

The problems of fault detection and isolation (FDI) and fault-tolerant control (FTC) in spacecraft attitude control system (ACS) for the gyro and star sensor (G&S) are addressed. The gyro and star sensor which measure the angular rate and the angular position respectively are the key components of ACS, and improvement to their accuracy and reliability contributes directly to the success of the mission of the spacecraft. The existing practical approaches mostly suppose either the gyro or the star sensor is fault-free; otherwise the measurement data fusion techniques[3-5] cannot remove the alternative fault or even make it worse than before. Since dual faults may well occur in G&S, it is necessary to design a framework taking the simultaneous faults into account in FDI/FTC.

Among the existing methods for fault diagnosis, model-based methods are the most popular and have received considerable attention in the past two decades. Many standard observer-based techniques exist in the literature providing different solutions to both the theoretical and practical aspects of the problem for the linear time-invariant (LTI) case[6-8]. In contrast to the LTI case, the spacecraft attitude control as a nonlinear problem lacks a universal approach and is currently an active area of research[9-11]. In this paper, the problem of FDI, which considers the uncertainty of the ASC caused by nonlinearity, can be converted into a classical H_∞ optimal control problem. Furthermore, we design two cascade observers using the cascaded relationship between the dynamics and kinematics of ACS[12-13]. This new structure is of significant practical interest:

· The FDI procedure is H_∞ optimal design oriented, which help application engineers to design FDI subsystem based on the mature H_∞ theory.

· Compared with a single observer, two cascade observers can separate a FDI design of ACS into a dynamics FDI design and a kinematics FDI design. It is convenient not only to more simply select suitable parameters, but also to better fit multiple working modes, e.g. attitude maneuver and attitude tracking.

· The cascade structure can transform the nonlinearity, unpredictable model uncertainty and diagnostic uncertainty into a uniform unknown input from system-inner to system-outer, where we can design a robust FDI system based on many regular fault diagnosis methods.

In this paper, the FDI problem for G&S of ACS is formulated using two cascades H_∞ optimal observers, which make the residual converge to the fault vector a-

Received 2010-10-08.

Sponsored by the National Natural Science Foundation of China (Grant No. 60774062), and the CAST Innovation Funding Project (Grant No. 20090604).

chieving detection and estimates at the same time. The first observer, using the extra degrees of freedom in the new structure to consider nonlinearity and model uncertainty, detects and estimates the gyro fault without angular position information. After that the second one utilized the estimates of angular velocity to make a robust diagnosis for the star sensor overcoming the impact of gyro diagnosis uncertainty. In addition, H_2 approach[14-16] is presented to reduce the false alarm rate of the designed observer and then a suitable trade-off between the sensitivity to sensor faults and the robustness to unknown inputs is also illustrated. Finally, simulation results verify the effectiveness to G&S dual faults, and a Compensation PD (CPD) controller is introduced to maintain ACS stability.

1 Spacecraft Model and Notations

The mathematical model of a rigid spacecraft can be derived by considering the equations describing the dynamics and kinematics of a rigid body. With reference to Ref. [17] for details, these equations are briefly recalled here.

$$\boldsymbol{J}\dot{\boldsymbol{\Omega}} = -[\boldsymbol{\Omega}^{\times}]\boldsymbol{J}\boldsymbol{\Omega} + \boldsymbol{u} \tag{1}$$

where $\boldsymbol{J} \in \mathbf{R}^{3\times3}$ denotes the symmetric inertia matrix, $\boldsymbol{\Omega} = [\Omega_1 \quad \Omega_2 \quad \Omega_3]^{\mathrm{T}} \in \mathbf{R}^3$ the spacecraft angular velocity and $\boldsymbol{u} = [u_1 \quad u_2 \quad u_3]^{\mathrm{T}} \in \mathbf{R}^3$ the control torques acting on the structure. We stress that all the equations are expressed in the body fixed frame. Define

$$[\boldsymbol{\Omega}^{\times}] = \begin{bmatrix} 0 & -\Omega_3 & \Omega_2 \\ \Omega_3 & 0 & -\Omega_1 \\ -\Omega_2 & \Omega_1 & 0 \end{bmatrix}$$

A common non-minimal parametrization usefully adopted for parametrizing the kinematics is that of the unitary quaternions, defined as

$$q_0 = \cos\frac{\theta}{2},\ q_i = e_i \sin\frac{\theta}{2},\ i = 1,2,3$$

with θ the rotation angle performed around the Euler's axis, specified by the unit vector with components e_i. Define $\boldsymbol{q} = [q_1 \quad q_2 \quad q_3]^{\mathrm{T}} \in R^3$. Obviously

$$\sum_{i=0}^{3} q_i^2 = 1 \tag{2}$$

The kinematics can be described as

$$\begin{bmatrix} \dot{q}_0 \\ \dot{\boldsymbol{q}} \end{bmatrix} = \frac{1}{2}\begin{bmatrix} [0 & -\Omega^{\mathrm{T}}] \\ R(\Omega) & \end{bmatrix}\begin{bmatrix} q_0 \\ \boldsymbol{q} \end{bmatrix} \tag{3}$$

with $R(\boldsymbol{\Omega}) = \begin{bmatrix} \Omega_1 & 0 & \Omega_3 & -\Omega_2 \\ \Omega_2 & -\Omega_3 & 0 & \Omega_1 \\ \Omega_3 & \Omega_2 & -\Omega_1 & 0 \end{bmatrix}$

Define $\boldsymbol{x}_g \triangleq \boldsymbol{\Omega}$, $\boldsymbol{x}_s \triangleq \boldsymbol{q}$, assume that system has stabilized in equilibrium $\boldsymbol{\Omega}_o$ which denotes the orbit angular velocity and consider the gyro fault $\boldsymbol{f}_g = [f_{g1} \quad f_{g2} \quad f_{g3}]^{\mathrm{T}} \in \mathbf{R}^3$ and the star sensor fault $\boldsymbol{f}_s = [f_{s1} \quad f_{s2} \quad f_{s3}]^{\mathrm{T}} \in \mathbf{R}^3$ to be detected. We eventually obtain the cascade model of the rigid spacecraft under fault conditions

$$\begin{aligned} \dot{\boldsymbol{x}}_g &= \boldsymbol{A}_g\boldsymbol{x}_g + \boldsymbol{B}_g\boldsymbol{u} \\ \boldsymbol{y}_g &= \boldsymbol{C}_g\boldsymbol{x}_g + \boldsymbol{f}_g \end{aligned} \tag{4}$$

$$\begin{aligned} \dot{\boldsymbol{x}}_s &= \boldsymbol{A}_s(\boldsymbol{x}_g)\boldsymbol{x}_s + \boldsymbol{E}_s(\boldsymbol{x}_g)\boldsymbol{\Phi}_s(\boldsymbol{x}_s) \\ \boldsymbol{y}_s &= \boldsymbol{C}_s\boldsymbol{x}_s + \boldsymbol{f}_s \end{aligned} \tag{5}$$

where

$$\boldsymbol{A}_g = -\boldsymbol{J}^{-1}[\boldsymbol{\Omega}_o^{\times}]\boldsymbol{J},\ \boldsymbol{B}_g = \boldsymbol{J}^{-1},\ \boldsymbol{C}_g = \boldsymbol{I}_3$$

$$\boldsymbol{A}_s(\boldsymbol{x}_g) = -\frac{1}{2}[\boldsymbol{x}_g^{\times}],\ \boldsymbol{E}_s(\boldsymbol{x}_g) = \frac{1}{2}\mathrm{diag}(\boldsymbol{x}_g),$$

$$\boldsymbol{\Phi}_s(\boldsymbol{x}_s) = \sqrt{1 - \sum_{i=1}^{3} q_i^2},\ \boldsymbol{C}_s = \boldsymbol{I}_3.$$

The first equation of Eq. (3) has not been considered since redundant. To this end, the following notations will be used.

Δ: The variable uncertainty operator.

Matrix $\boldsymbol{I}_n$: the identity matrix of order n.

Matrix $\boldsymbol{0}_n$: the zero square matrix of order n.

Matrix $\boldsymbol{0}_{nm}$: the zero $n \times m$ matrix.

$\mathrm{diag}_n(a)/\mathrm{diag}(a)$: the diagonal square matrix of order n with $[a \cdots a]_{1\times n}$ as its diagonal vector, or the one with a as its diagonal vector.

$\hat{T}_{yu}$: the transfer matrix from input u to output y.

RH_∞: the space of all proper real rational stable transfer matrices.

Matrix $H(s) = \left[\begin{matrix} A & B \\ C & D \end{matrix}\right]$, when used in $y = H(s)u$:

$$\begin{aligned} \dot{\xi} &= A\xi + Bu,\ y = C\xi + Du \\ H(s) &= C(sI - A)^{-1}B + D. \end{aligned}$$

The setup will also be used throughout the paper along with

$$\boldsymbol{G} = \begin{bmatrix} \boldsymbol{A} & \boldsymbol{B}_1 & \boldsymbol{B}_2 \\ \boldsymbol{C}_1 & \boldsymbol{D}_{11} & \boldsymbol{D}_{12} \\ \boldsymbol{C}_2 & \boldsymbol{D}_{21} & \boldsymbol{D}_{22} \end{bmatrix} \tag{6}$$

We will also utilize the following result from Ref. [18].

Theorem 1 Assume stabilizability and detectability of $(\boldsymbol{A}, \boldsymbol{B}_2, \boldsymbol{C}_2)$ and that $\boldsymbol{D}_{22} = \boldsymbol{0}$ and let $\boldsymbol{N}_r$ and $\boldsymbol{N}_s$ denote orthonormal bases of the null spaces of $(\boldsymbol{B}_2^{\mathrm{T}}, \boldsymbol{C}_{12}^{\mathrm{T}})$ and $(\boldsymbol{C}_2, \boldsymbol{D}_{21})$. There exists a controller K such that $\|\boldsymbol{T}_{yu}\|_\infty < \gamma$ iff there exist symmetric $\boldsymbol{R}, \boldsymbol{S} \in \mathbf{R}^{n\times n}$ satisfying the following system of LMIs

$$\begin{pmatrix} \boldsymbol{N}_r & \boldsymbol{0} \\ \boldsymbol{0} & \boldsymbol{I} \end{pmatrix}^{\mathrm{T}} \begin{pmatrix} \boldsymbol{AR} + \boldsymbol{RA}^{\mathrm{T}} & \boldsymbol{RC}_1^{\mathrm{T}} & \boldsymbol{B}_1 \\ \boldsymbol{C}_1\boldsymbol{R} & -\gamma\boldsymbol{I} & \boldsymbol{D}_{11} \\ \boldsymbol{B}_1^{\mathrm{T}} & \boldsymbol{D}_{11}^{\mathrm{T}} & -\gamma\boldsymbol{I} \end{pmatrix} \begin{pmatrix} \boldsymbol{N}_r & 0 \\ 0 & \boldsymbol{I} \end{pmatrix} < 0 \tag{7}$$

$$\begin{pmatrix} \boldsymbol{N}_s & \boldsymbol{0} \\ \boldsymbol{0} & \boldsymbol{I} \end{pmatrix}^{\mathrm{T}} \begin{pmatrix} \boldsymbol{AS} + \boldsymbol{SA}^{\mathrm{T}} & \boldsymbol{SB}_1 & \boldsymbol{C}_1^{\mathrm{T}} \\ \boldsymbol{B}_1^{\mathrm{T}}\boldsymbol{S} & -\gamma\boldsymbol{I} & \boldsymbol{D}_{11}^{\mathrm{T}} \\ \boldsymbol{C}_1 & \boldsymbol{D}_{11} & -\gamma\boldsymbol{I} \end{pmatrix} \begin{pmatrix} \boldsymbol{N}_s & \boldsymbol{0} \\ \boldsymbol{0} & \boldsymbol{I} \end{pmatrix} < 0 \tag{8}$$

$$-\begin{pmatrix} \boldsymbol{R} & \boldsymbol{I} \\ \boldsymbol{I} & \boldsymbol{S} \end{pmatrix} < 0 \tag{9}$$

2 H_∞ Optimal Fault Observer for Gyros

In this section, the H_∞ optimal fault observer for gyros will be designed. According to Eq. (4), the following observer structure is adopted, by making use of the dynamical observer as

$$\begin{aligned} \dot{\hat{\boldsymbol{x}}}_g &= \boldsymbol{A}_g\hat{\boldsymbol{x}}_g + \boldsymbol{B}_g\boldsymbol{u} + \boldsymbol{\eta}_g \\ \hat{\boldsymbol{y}}_g &= \boldsymbol{C}_g\hat{\boldsymbol{x}}_g \end{aligned} \tag{10}$$

$$\begin{aligned} \dot{\boldsymbol{\xi}}_g &= \boldsymbol{A}_{gL}\boldsymbol{\xi}_g + \boldsymbol{B}_{gL}(\boldsymbol{y}_g - \hat{\boldsymbol{y}}_g) \\ \boldsymbol{\eta}_g &= \boldsymbol{C}_{gL}\boldsymbol{\xi}_g + \boldsymbol{D}_{gL}(\boldsymbol{y}_g - \hat{\boldsymbol{y}}_g) \end{aligned} \tag{11}$$

where $\boldsymbol{A}_{gL} \in \mathbf{R}^{3\times3}$, $\boldsymbol{B}_{gL} \in \mathbf{R}^{3\times3}$, $\boldsymbol{C}_{gL} \in \mathbf{R}^{3\times3}$, $\boldsymbol{D}_{gL} \in \mathbf{R}^{3\times3}$.

We will write $\boldsymbol{K}_g(s) = \begin{bmatrix} \boldsymbol{A}_{gL} & \boldsymbol{B}_{gL} \\ \boldsymbol{C}_{gL} & \boldsymbol{D}_{gL} \end{bmatrix}$ to represent the dynamical observer gain in Eq. (10).

Define the state estimate error $\boldsymbol{e}_g = \boldsymbol{x}_g - \hat{\boldsymbol{x}}_g$ and the output estimate erro $\boldsymbol{r}_g = \boldsymbol{y}_g - \hat{\boldsymbol{y}}_g$, so it follows Eqs. (4) and (10) that

$$\begin{aligned} \dot{\boldsymbol{e}}_g &= [\boldsymbol{A}_g - \boldsymbol{K}_g(s)\boldsymbol{C}_g]\boldsymbol{e}_g - \boldsymbol{K}_g(s)\boldsymbol{f}_g \\ \tilde{\boldsymbol{y}}_g &= \boldsymbol{C}_g\boldsymbol{e}_g + \boldsymbol{f}_g \end{aligned} \tag{12}$$

From Eq. (12), it is clear that by scheming $\boldsymbol{K}_g(s)$ so as to minimize the state estimate error $\boldsymbol{e}_g$, the output estimate error $\tilde{\boldsymbol{y}}_g$ converges to $\boldsymbol{f}_g$ which guarantees fault identification as well as

$$\tilde{\boldsymbol{y}}_g = \underset{\boldsymbol{e}_g(\boldsymbol{K}_g(s),\boldsymbol{f}_g)\to0}{Optimum}(\boldsymbol{C}_g\boldsymbol{e}_g + \boldsymbol{f}_g) \approx \boldsymbol{f}_g \tag{13}$$

It can be seen that Eq. (13) belongs to a single-object optimal problem which can be easily achieved. The dynamical observer function in Eq. (12) is now given which can be represented by the following standard form

$$\dot{\boldsymbol{e}}_g = \boldsymbol{A}_g\boldsymbol{e}_g + [\boldsymbol{0}_3 \quad -\boldsymbol{I}_3]\begin{bmatrix} \boldsymbol{f}_g \\ \boldsymbol{\nu}_g \end{bmatrix} \tag{14}$$

$$\begin{bmatrix} \boldsymbol{z}_g \\ \tilde{\boldsymbol{y}}_g \end{bmatrix} = \begin{bmatrix} \boldsymbol{I}_3 \\ \boldsymbol{C}_g \end{bmatrix}\boldsymbol{e}_g + \begin{bmatrix} \boldsymbol{0}_3 & \boldsymbol{0}_3 \\ \boldsymbol{I}_3 & \boldsymbol{0}_3 \end{bmatrix}\begin{bmatrix} \boldsymbol{f}_g \\ \boldsymbol{\nu}_g \end{bmatrix} \tag{15}$$

where

$$\begin{aligned} \boldsymbol{\nu}_g &= \boldsymbol{K}_g(s)(\boldsymbol{y}_g - \hat{\boldsymbol{y}}_g) \\ \boldsymbol{z}_g &= \boldsymbol{e}_g = \boldsymbol{x}_g - \hat{\boldsymbol{x}}_g. \end{aligned}$$

The following theorem gives the observer asymptotic convergence result on fault identification problem of the spacecraft gyros:

Theorem 2 For the observer given by Eq. (10) along with $\tilde{\boldsymbol{y}}_g$ is an optimal residual generator for the gyro fault diagnosis problem if the dynamical gain $\boldsymbol{K}_g(s) \in \mathbf{R}H_\infty$ (the set of controllers solving the H_∞ optimal control problem with the minimum possible γ) exists.

3 H_∞ Optimal Fault Observer for Star Sensor

The fault diagnosis architecture of the star sensor basically resembles the gyro. However, it is important to note that the following assumptions are taken for the observer's design of the star sensor.

A1: The fault $\boldsymbol{f}_s$ is sectionally continuous.

A2: The measured value always satisfies normalization condition even though faults happened. That means

$$\sum_{i=1}^{3}(q_i + f_{si})^2 + q_0^2 = 1 \tag{16}$$

A3: When the estimate error of the angular rate exists and keeps bounded by Eq. (10), the estimate of the angular position here also remains of errors and bounded. Consequently, there is a real number α such that

$$\|\boldsymbol{e}_g\|_2 = \|\boldsymbol{x}_g - \hat{\boldsymbol{x}}_g\|_2 \leqslant \alpha\|\boldsymbol{x}_s - \hat{\boldsymbol{x}}_s\|_2 \tag{17}$$

A4: There exists a positive number α_Φ such that $\boldsymbol{\Phi}_s(\boldsymbol{x}_s)$ satisfies a Lipschitz condition i. e.

$$\|\boldsymbol{\Phi}_s(\boldsymbol{x}_s) - \boldsymbol{\Phi}_s(\hat{\boldsymbol{x}}_s)\|_2 \leqslant \alpha_\Phi\|\boldsymbol{x}_s - \hat{\boldsymbol{x}}_s\|_2 \tag{18}$$

Remark 1 A1 provides a guarantee that the form of star sensor faults can be described by mathematics. A2 satisfies the fault dimension equivalence between the Euler angle and the unit quaternion. Taking the gyro observer diagnosis uncertainty and system nonlinearity into consideration refer to A3 and A4 when we design the star sensor observer.

Based on above assumption and according to Eq. (5), the fault observer of star sensors proposed falls in the class of the Luenberger-like observer, namely

$$\begin{aligned} \dot{\hat{\boldsymbol{x}}}_s &= \boldsymbol{A}_s(\hat{\boldsymbol{x}}_g)\hat{\boldsymbol{x}}_s + \boldsymbol{E}_s(\hat{\boldsymbol{x}}_g)\boldsymbol{\Phi}_s(\hat{\boldsymbol{x}}_s) + \boldsymbol{K}_s(s)(\boldsymbol{y}_s - \hat{\boldsymbol{y}}_s) \\ \hat{\boldsymbol{y}}_s &= \boldsymbol{C}_s\hat{\boldsymbol{x}}_s \end{aligned} \tag{19}$$

where $\hat{\boldsymbol{x}}_g$ replaces $\boldsymbol{x}_g$ in matrices $\boldsymbol{A}_s(\hat{\boldsymbol{x}}_g)$ and $\boldsymbol{E}_s(\hat{\boldsymbol{x}}_g)$ in view of the inequality between measured value $\boldsymbol{y}_g$ and real states $\boldsymbol{x}_g$ considering the gyro fault may happen at all times. Thus matrices $\boldsymbol{A}_s(\hat{\boldsymbol{x}}_g)$ and $\boldsymbol{E}_s(\hat{\boldsymbol{x}}_g)$ can be expressed as

$$\begin{aligned} \boldsymbol{A}_s(\hat{\boldsymbol{x}}_g) &= \boldsymbol{A}_s(\boldsymbol{x}_g) + \boldsymbol{\Delta}_A \\ \boldsymbol{E}_s(\hat{\boldsymbol{x}}_g) &= \boldsymbol{E}_s(\boldsymbol{x}_g) + \boldsymbol{\Delta}_E \end{aligned} \tag{20}$$

with $\boldsymbol{\Delta}_A = -\frac{1}{2}[\boldsymbol{e}_g^\times]$, $\boldsymbol{\Delta}_E = \frac{1}{2}\mathrm{diag}(\boldsymbol{e}_g)$.

According to A3, there exist positive real numbers α_A and α_E such that above matrices satisfy a local Lipschitz condition

$$\begin{aligned} \|\boldsymbol{\Delta}_A\|_2 &= \|\boldsymbol{A}_s(\boldsymbol{x}_g) - \boldsymbol{A}_s(\hat{\boldsymbol{x}}_g)\|_2 \leqslant \alpha_A\|\boldsymbol{x}_s - \hat{\boldsymbol{x}}_s\|_2 \\ \|\boldsymbol{\Delta}_E\|_2 &= \|\boldsymbol{E}_s(\boldsymbol{x}_g) - \boldsymbol{E}_s(\hat{\boldsymbol{x}}_g)\|_2 \leqslant \alpha_E\|\boldsymbol{x}_s - \hat{\boldsymbol{x}}_s\|_2 \end{aligned} \tag{21}$$

Also define $\boldsymbol{e}_s = \boldsymbol{x}_s - \hat{\boldsymbol{x}}_s$ and $\tilde{\boldsymbol{y}}_s = \boldsymbol{y}_s - \hat{\boldsymbol{y}}_s$. From Eqs. (5), (19) and (20) that

$$\begin{aligned} \dot{\boldsymbol{e}}_s &= \boldsymbol{A}_s(\boldsymbol{x}_g)\boldsymbol{x}_s + \boldsymbol{E}_s(\boldsymbol{x}_g)\boldsymbol{\Phi}_s(\boldsymbol{x}_s) - \boldsymbol{A}_s(\hat{\boldsymbol{x}}_g)\hat{\boldsymbol{x}}_s - \boldsymbol{E}_s(\hat{\boldsymbol{x}}_g)\boldsymbol{\Phi}_s(\hat{\boldsymbol{x}}_s) - \boldsymbol{K}_s(s)(\boldsymbol{C}_s\boldsymbol{e}_s + \boldsymbol{f}_s) = [\boldsymbol{A}_s(\hat{\boldsymbol{x}}_g) - \boldsymbol{K}_s(s)\boldsymbol{C}_s]\boldsymbol{e}_s - \boldsymbol{K}_s(s)\boldsymbol{f}_s + \boldsymbol{\Delta}_{\text{total}} \\ \tilde{\boldsymbol{y}}_s &= \boldsymbol{C}_s\boldsymbol{e}_s + \boldsymbol{f}_s \end{aligned} \tag{22}$$

$$\boldsymbol{\Delta}_{\text{total}} = \boldsymbol{E}_s(\hat{\boldsymbol{x}}_g)[\boldsymbol{\Phi}_s(\boldsymbol{x}_s) - \boldsymbol{\Phi}_s(\hat{\boldsymbol{x}}_s)] + [\boldsymbol{\Delta}_A\hat{\boldsymbol{x}}_s + \boldsymbol{\Delta}_E\boldsymbol{\Phi}_s(\hat{\boldsymbol{x}}_s)]$$

Since $\Phi_s(x_s)$, Δ_A and Δ_E all satisfy the Lipschitz condition according to A4 and Eq. (21), $E_s(x_g)$, $\hat{x}_s$ and $\Phi_s(\hat{x}_s)$ are obviously bounded. We deduce that Δ_{total} corresponds with Lipschitz condition as well

$$\| \Delta_{\text{total}} \|_2 \leqslant \alpha_{\text{total}} \| x_s - \hat{x}_s \|_2 \tag{23}$$

where α_{total} is a positive real number.

The following lemma from Ref. [19] gives the asymptotic convergence condition of the H_∞ observer.

Lemma 1 The observer gain $K_s(s)$ stabilizes the error dynamics for all Δ_{total} with a Lipschitz constant α_{total} if $K_s(s)$ is chosen so as to ensure that it can be related to the H_∞ theory such that

$$\sup_{\omega \in R} \sigma_{\max} [T_{z\Delta_{\text{total}}}(j\omega)] < \frac{1}{\alpha_{\text{total}}} \tag{24}$$

Citing Lemma 1, above fault problem looks more complicated because it needs the designed observer not only to minimize the state estimate error, but also to guarantee some robustness suitable for uncertainties.

Define $\tau_s \triangleq [\tau_{s1} \quad \tau_{s2}]^{\mathrm{T}} = [\Delta_{\text{total}} \quad f_s]^{\mathrm{T}}$, it can be seen that the dynamical observer function in Eq. (22) is now given which can be represented by the following standard form

$$\dot{e}_s = A_s e_s + [[I_3 \quad 0_3] \quad -I_3] \begin{bmatrix} \tau_s \\ \nu_s \end{bmatrix} \tag{25}$$

$$\begin{bmatrix} z_s \\ \tilde{y}_s \end{bmatrix} = \begin{bmatrix} I_3 \\ C_s \end{bmatrix} e_s + \begin{bmatrix} [0_3 & 0_3] & 0_3 \\ [0_3 & I_3] & 0_3 \end{bmatrix} \begin{bmatrix} \tau_s \\ \nu_s \end{bmatrix} \tag{26}$$

where

$$\nu_s = K_s(s)(y_s - \hat{y}_s)$$
$$z_s = e_s = x_s - \hat{x}_s.$$

Finally, the following theorem describes the fault diagnosis problem of the star sensor as

Theorem 3 Given system (5), the residual $\tilde{y}_s$ achieves the fault diagnosis if the dynamical gain $K_s(s) \in \mathbf{RH}_\infty$ exists and satisfies $\| T_{e_s \Delta_{\text{total}}} \|_\infty < \frac{1}{\alpha_{\text{total}}}$ and $\| T_{ef_s} \|_\infty$ the minimum possible.

4 LMI Design Procedure for G&S

Before LMI design, we reconsider the model of the dynamics Eq. (4). In practice, symmetric inertia matrix J exist some uncertainty Δ_J. In addition, the disturbance torque supposed due to the gravity-gradient is non-ignorable. Hence, we assume uncertainty item $\Psi(x_g, \Delta_J, x_s)$ also matches the Lipschitz condition and the dynamics is rewritten as follows

$$\dot{x}_g = A_g x_g + \Psi(x_g, \Delta_J, x_s) + B_g u$$
$$y_g = C_g x_g + f_g \tag{27}$$

Define $\tau_g \triangleq [\tau_{g1} \quad \tau_{g2}]^{\mathrm{T}} = [\Psi(x_g, \Delta_J, x_s) \quad f_g]^{\mathrm{T}}$ and the standard form is rewritten by

$$\dot{e}_g = A_g e_g + [[I_3 \quad 0_3] \quad -I_3] \begin{bmatrix} \tau_g \\ \nu_g \end{bmatrix} \tag{28}$$

$$\begin{bmatrix} z_g \\ \tilde{y}_g \end{bmatrix} = \begin{bmatrix} I_3 \\ C_g \end{bmatrix} e_g + \begin{bmatrix} [0_3 & 0_3] & 0_3 \\ [0_3 & I_3] & 0_3 \end{bmatrix} \begin{bmatrix} \tau_g \\ \nu_g \end{bmatrix} \tag{29}$$

Eqs. (25) – (26) and Eqs. (28) – (29) all satisfy a uniform structure so that we can design the observer of the gyro and star sensor together (omit subscript g and s) and the general plant can be given as

$$G(s) = \begin{bmatrix} A & [I_3 & 0_3] & -I_3 \\ I_3 & [0_3 & 0_3] & 0_3 \\ C & [0_3 & I_3] & 0_3 \end{bmatrix} \tag{30}$$

As stated in Theorem 2, minimizing $\| T_{ef} \|_\infty$ possible can be modeled as a weighted H_∞ problem solvable using the dynamical observer formulation and then the following two statements are equivalent

(i) $\hat{T}_{ef}(j\omega) = 0$.

(ii) $W(s)\hat{T}_{ef}(j\omega) \in \mathbf{RH}_\infty$. (31)

According to Theorem 3, we know the scheme belongs to a kind of H_∞ multi-evaluation problem. In order to balance such two-objective values, a positive scalar ε is used with the second objective such that

$$\varepsilon \| W(s) T_{ef} \| < 1/\alpha \tag{32}$$

It then follows that $\| T_{e\Delta} \|_\infty$ and $\| T_{ef} \|_\infty$ can be combined in a uniform framework, and with the weighting $W(s)$ defined as follows

$$W(s) = \begin{bmatrix} A_\omega & B_\omega \\ C_\omega & D_\omega \end{bmatrix} \tag{33}$$

It can be seen that the augmented plant $\bar{G}(s)$ is given by

$$\bar{G}(s) = \begin{bmatrix} \begin{bmatrix} A_\omega & 0_3 \\ 0_3 & A \end{bmatrix} & \begin{bmatrix} 0_3 & B_\omega \\ I_3 & 0_3 \end{bmatrix} & \begin{bmatrix} 0_3 \\ -I_3 \end{bmatrix} \\ [0_3 \quad I_3] & [0_3 \quad 0_3] & 0_3 \\ [\varepsilon C_\omega \quad C] & [0_3 \quad \varepsilon D_\omega] & 0_3 \end{bmatrix} \tag{34}$$

Given faults are low frequency signals, A_ω, B_ω, C_ω and D_ω are designed as

$$A_\omega = \mathrm{Diag}_3(-c), B_\omega = I_3$$
$$C_\omega = \mathrm{Diag}_3(b - ac), D_\omega = \mathrm{Diag}_3(a) \tag{35}$$

where the positive number b is related to the fault upper frequency $\omega_{\max}$; positive a and c are both small numbers which guarantee LMI solvable.

Based on the previous results, the following theorem summarizes the sensor fault diagnosis problem:

Theorem 4 Given the observer form like Eq. (19), there exist optimal residual $\tilde{y}$ estimating the fault of G&S according to theorem 3, for all uncertainty Δ satisfying with a Lipschitz condition iff $\exists \varepsilon > 0$ and a controller $K(s)$ design by Theorem 1 satisfying $\| T_{e\tau} \|_\infty < \frac{1}{\alpha}$ for the structure where $\bar{G}(s)$ has the state space representation in Eq. (34).

5 Robust Residual Evaluation

In practice, there are usually such a great number

of unknown inputs that, in the face of mismatching the Lipschitz condition, a complete decoupling from all unknown inputs is hardly achievable. Hence the residuals or any decision functions built from them always deviate from zero even if no fault is present. In this case, robust residual evaluation is the only way to keep the false alarm rate small with an acceptable sensitivity to faults. Here, we adopt H_2 approach[14-16] to analyze the robustness of the designed gyro observer in frequency domain.

Consider unknown inputs $\boldsymbol{d} = [d_1 \quad d_2 \quad d_3]^{\mathrm{T}} \in \mathbf{R}^3$, so the dynamics of ACS is rewritten such as

$$\begin{aligned} \dot{\boldsymbol{x}}_g &= \boldsymbol{A}_g \boldsymbol{x}_g + \boldsymbol{B}_g \boldsymbol{u} + d \\ \boldsymbol{y}_g &= \boldsymbol{C}_g \boldsymbol{x}_g + \boldsymbol{f}_g \end{aligned} \tag{36}$$

Follow Eqs. (10) and (36) that we acquire transfer matrices from d or $\boldsymbol{f}_g$ to $\tilde{\boldsymbol{y}}_g$ as

$$\tilde{\boldsymbol{y}}_g = \boldsymbol{\Gamma}_d \boldsymbol{d} + \boldsymbol{\Gamma}_f \boldsymbol{f}_g \tag{37}$$

where

$$\begin{aligned} \boldsymbol{\Gamma}_d &= \boldsymbol{C}_g (s\boldsymbol{I}_3 - \bar{\boldsymbol{A}})^{-1} \\ \boldsymbol{\Gamma}_f &= \boldsymbol{C}_g (s\boldsymbol{I}_3 - \bar{\boldsymbol{A}})^{-1} \boldsymbol{K}_g(s) + \boldsymbol{I}_3 \\ \bar{\boldsymbol{A}} &= \boldsymbol{A}_g + \boldsymbol{K}_g(s) \boldsymbol{C}_g \end{aligned}$$

According to Section 5, we know that $\bar{\boldsymbol{A}}$ has been stabilizing, hence a dynamics of residual evaluation is governed by

$$r(s) = \boldsymbol{R}(s)(\boldsymbol{\Gamma}_d \boldsymbol{d} + \boldsymbol{\Gamma}_f f_g) \tag{38}$$

where $\boldsymbol{R}(s) \in \mathbf{RH}_\infty^{1\times m}$ is called post-filter. In case that a full decoupling is not achievable, the design goal is to find a residual generator such that the H_2 performance index J_{opt} becomes minimal. Using Eq. (37), J_{opt} can be express as

$$J_{\mathrm{opt}} = \min_{\boldsymbol{R}(s) \in \mathbf{RH}_\infty^{1\times m}} \frac{\| \boldsymbol{R}(s) \boldsymbol{\Gamma}_d \|_2}{\| \boldsymbol{R}(s) \boldsymbol{\Gamma}_f \|_2} \tag{39}$$

The minimization leads to a generalized eigenvalue-eigenvector problem i. e.

$$\boldsymbol{p}(i\omega)[(\boldsymbol{\Gamma}_d(i\omega)\boldsymbol{\Gamma}_d^*(i\omega) - \boldsymbol{\sigma}_{\min}(\omega)\boldsymbol{\Gamma}_f(i\omega) \cdot \boldsymbol{\Gamma}_f^*(i\omega)] = 0 \tag{40}$$

$\boldsymbol{\sigma}_{\min}(\omega)$ and $\boldsymbol{p}(i\omega)$ are, respectively, the minimal generalized eigenvalue and corresponding eigenvector. The solution to this problem in the frequency domain finally yields

$$\begin{aligned} \boldsymbol{R}_{\mathrm{opt}}(s) &= f_{\omega_0}(s) \boldsymbol{p}(s), \\ J_{\mathrm{opt}} &= \inf_{\omega} \boldsymbol{\sigma}_{\min}(\omega) \end{aligned} \tag{41}$$

and ω_0 is the frequency at which $\boldsymbol{\sigma}_{\min}(\omega)$ achieves its minimum. $f_{\omega_0}(s)$ denotes an ideal frequency-selective filter at ω_0, which can be replaced by a narrow band filter

$$f_{\omega_0}(s) = \frac{\lambda s^\beta}{(s + \omega_0)^{2\beta}} \tag{42}$$

where positive number λ determines the magnitude of the signal and integer β are used to adjust a desirable bandwidth.

In general, a conservative threshold[14] can be, according to Eq. (37), established as follows

$$J_{th} = 2 \sup_{f_g = 0} \| r(s) \|_2 \tag{43}$$

and the robust fault detection and isolation problem of the gyro observer for unknown inputs can be expressed by

$$\begin{aligned} \| r(s) \|_2 < J_{th} &\rightarrow \text{sensor fault-free} \\ \| r(s) \|_2 \geqslant J_{th} &\rightarrow \text{sensor faulty} \end{aligned} \tag{44}$$

6 Compensation PD Fault-Tolerant Control

In the previous sections, the FDI architecture on G&S has been represented. Their residuals $\tilde{y}_g$ and $\tilde{y}_s$ asymptotically converge to fault vectors f_g and f_s respectively. Hence, through measurement values minus their residuals, a compensation PD (CPD) feedback controller is given as follows

$$\boldsymbol{u} = \boldsymbol{K}_p(\boldsymbol{y}_s - \tilde{\boldsymbol{y}}_s) + \boldsymbol{K}_d(\boldsymbol{y}_g - \tilde{\boldsymbol{y}}_g) \tag{45}$$

where the controller parameters $\boldsymbol{K}_p$ and $\boldsymbol{K}_d$ can be deduced using the root locus analysis. We set CPD open when residual evaluation r climbs across the threshold, otherwise a general PD controller acts. Fig. 1 illustrates the structure of the close-loop system including spacecraft plant, fault diagnosis subsystem and CPD controller.

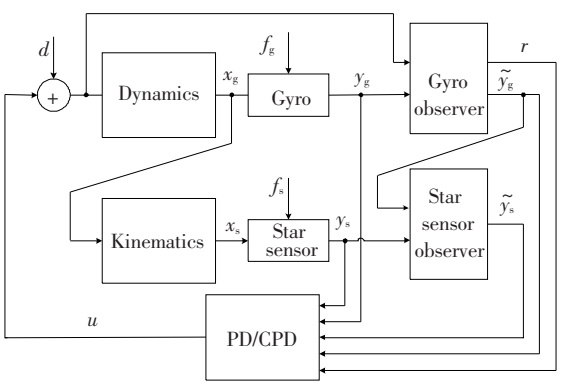

Fig. 1 Structure of cascade observers and control system

7 Simulation Results and Discussions

In this section, the spacecraft simulation involves an earth orientation attitude regulation. Here we consider system existing actuator disturbance signals, G&S noises and assume them as white noises whose standard deviations are denoted by σ. With reference to Ref. [20], the parameters of the simulated rigid spacecraft and circumstance including model uncertainty and unknown inputs are given in 0To conquer both uncertainties and disturbances, a suitable parameter ε can be selected e. g. by simulation tests or application experiences.

In the benchmark, a couple of fiber gyro and star sensor are addressed and then two typical faults in

practice are listed in 0Simplifying the results, here two scenarios including a periodic additive fault of fiber gyro and a constant additive fault of star sensor are shown to illustrate the performance of FDI/FTC system when operating together.

Scenario 1 Gyro and star sensor faults simultaneously occur at time $t = 30$ (s) as

$$\boldsymbol{f}_g = \begin{bmatrix} 0.05\sin(0.1t) \\ 0.01\sin(0.5t + \pi/4) \\ 0.03 + 0.01\sin(t) \end{bmatrix} (\text{rad/s}), \boldsymbol{f}_s = \begin{bmatrix} 0.4 \\ 0.5 \\ 0.6 \end{bmatrix}$$

Tab. 1 Model parameters and value

Symbol	Quantity
SP, MU and UI	$J = \begin{bmatrix} 55.30 & 0.21 & 0.41 \\ 0.21 & 51.50 & -0.34 \\ 0.41 & -0.34 & 41.80 \end{bmatrix} (\text{kg} \cdot \text{m}^2)$, $\sigma_g = 2 \times 10^{-4} (\text{rad/s})$ $\Delta_J = \begin{bmatrix} 27.6\sin(0.02t) & 0.105\cos(0.01t) & 0.205\sin(0.02t) \\ 0.105\cos(0.01t) & 25.7\cos(0.02t) & -0.17\cos(0.01t) \\ 0.205\sin(0.02t) & -0.17\cos(0.01t) & 20.9\sin(0.02t) \end{bmatrix} (\text{kg} \cdot \text{m}^2)$ $\Omega_o = [0 \quad -0.001 \quad 0]^{\mathrm{T}} (\text{rad/s})$, $\Omega_{\text{initial}} = [0 \quad 0 \quad 0]^{\mathrm{T}} (\text{rad/s})$ $q_{\text{initial}} = [1 \quad 0 \quad 0 \quad 0]^{\mathrm{T}}$, $\sigma_s = 2 \times 10^{-4}$, $\sigma_a = 0.7$ (μN · m) $d = \begin{bmatrix} -4 + 5\cos(0.01t) \\ 4 + 3\sin(0.01t) \\ -4 + 4\sin(0.01t) \end{bmatrix} \times 10^{-4}$ (N · m)
WP, FP	$b = 5$, $a = 1 \times 10^{-6}$, $c = 1 \times 10^{-2}$, $\lambda = 8$, $\beta = 2$, $\varepsilon = 1 \times 10^2$
CPD	$K_p = 150$, $K_d = 100$

SP: spacecraft parameter; MU: model uncertainty; UI: unknown input; FP: filter parameter; WP: weighting parameter

Tab. 2 Two typical faults of G&S

Component	Abnormality	Failure cause	Faulty form
Star sensor	Attitude information locked	Timing generator abnormal	A constant additive fault
Fiber gyro	Light power unstable	Constant-current source unstable	A periodical fault signals

To illustrate the performance and the feasibility of two H_∞ fault observers and CPD controller, fault estimates, errors of fault estimates, the control torque, the angular rate and angular position are presented from Figs. 2 to 8. G&S fault estimates and their errors in scenario 1 are plotted in Figs. 2 – 5.

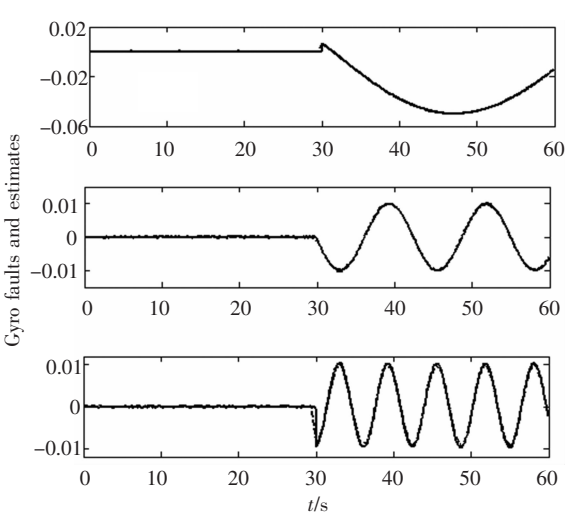

Fig. 2 Gyro faults and Estimates in Scenario 1

We can see that each error of the G&S fault vector converges to a small set around the zero point with noise order and maintains still bounded in this area even though G&S dual faults occur. In addition, the results also verify that the cascade observers in design have the robustness with respect to model uncertainties and unknown inputs.

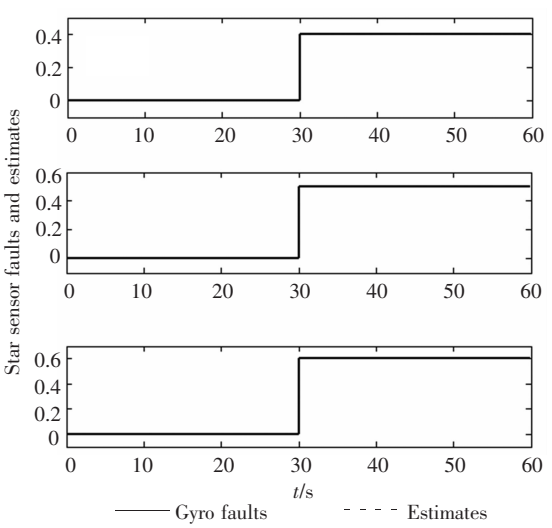

Fig. 3 Star sensor faults and estimates in Scenario 1

Based on the support of above accurate and delay-free diagnosis results, CPD controller can rapidly eliminate the impact of G&S faults on ACS. Different to Bias-Separated Filters[3], the new cascade structure is totally independent on star sensor signals so that it is a-

ble to identify gyro faults and star sensor faults simultaneously. In fact, a perfect identification of G&S fault in this framework relies on the accurate input signals. It is well-known that in the space environment, the unknown inputs and disturbances are usually relatively weak compared with control inputs. Therefore, it shows that the above cascade observers can be designed and achieved. Finally, we plot real angular velocity, unit quaternion and control torque of ACS in Figs. 6-8 respectively to show the effectiveness of this FDI/FTC.

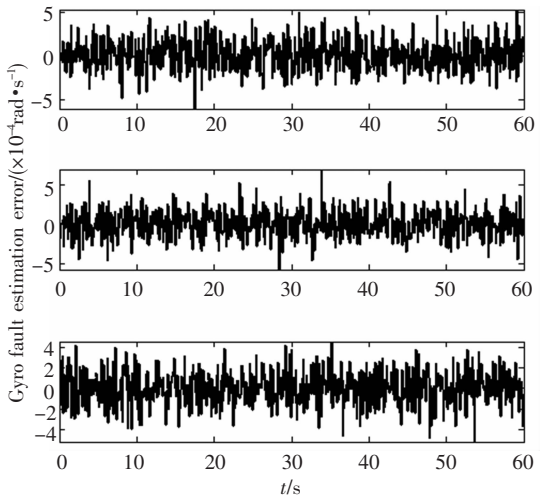

Fig. 4 Gyro fault estimation errors in Scenario 1

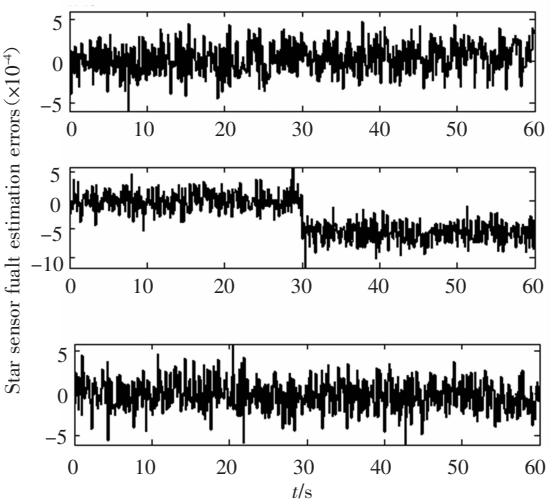

Fig. 5 Star sensor fault estimation errors in Scenario 1

Scenario 2 Only gyro fault occurs at time t = 30 (s) but this time its magnitude becomes as weak as unknown disturbances d:

$$f_g = d = \begin{bmatrix} -4 + 5\cos(0.01t) \\ 4 + 3\sin(0.01t) \\ -4 + 4\sin(0.01t) \end{bmatrix} \times 10^{-4}(\text{rad/s})$$

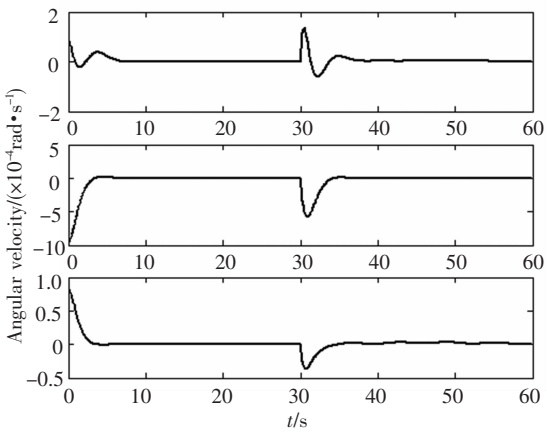

Fig. 6 Real angular velocity in Scenario 1

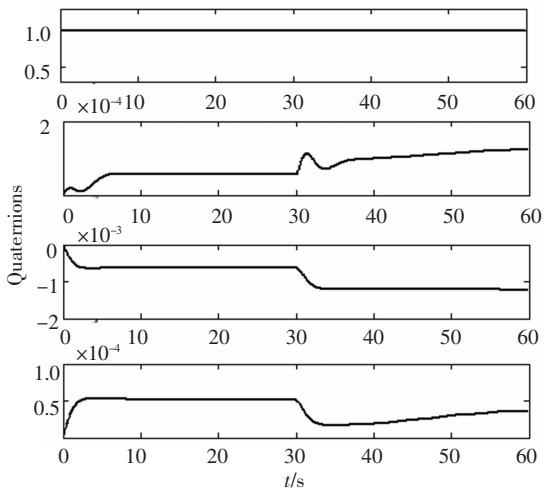

Fig. 7 Real quaternions in Scenario 1

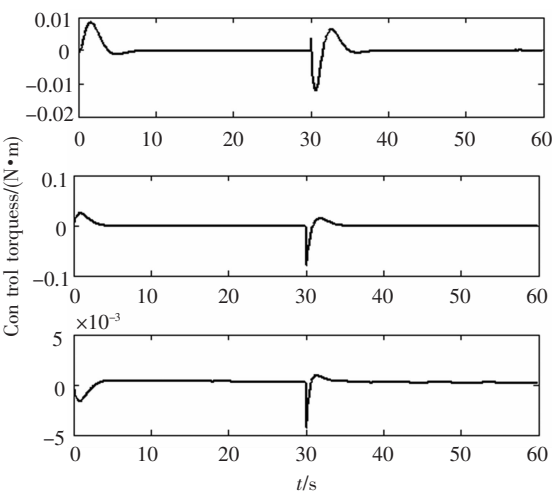

Fig. 8 Control torques in Scenario 1

Relationship between J and ω is presented as numerical analysis using the H_2 approach. Fig. 9 demonstrates the performance index J becomes smaller and smaller with the increase of frequency and it is obviously logical because transfer matrix Γ_f has direct output

but Γ_d not. However, selecting an excessively high frequency may lead to miss detection correspondingly when filters weaken low frequency information of gyro faults as the same as unknown inputs. Therefore, a suitable trade-off between the sensitivity to sensor faults and the robustness to unknown inputs is necessary in practice. Here according to Fig. 9 and the frequency of faults, we select $\omega_0 = 1$ as the center frequency of the band filter and its parameters are also listed in 0.

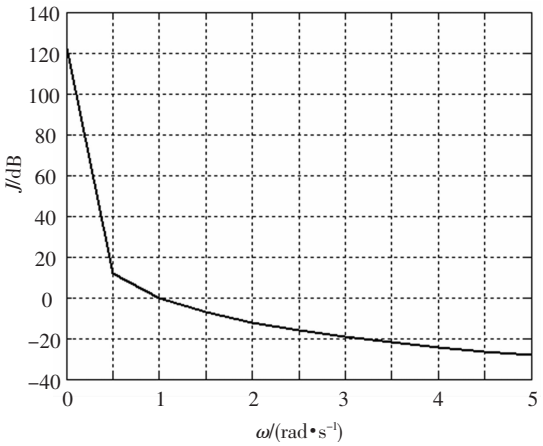

Fig. 9 Relationship between frequency and performance

Residual $\tilde{y}$ and its threshold in Scenario 2 are both shown in Fig. 10, which shows that the impact of gyro fault is totally covered below the threshold such that miss detection occurs. Compared with the results in Fig. 10, Fig. 11 shows that the filtered detection residualrin the pitch and yaw axis well crosses the threshold indicated by the dashed lines. This comparative experiment means the size of minimum detectable faults for cascade observers has been minimized and robust diagnosis achieved.

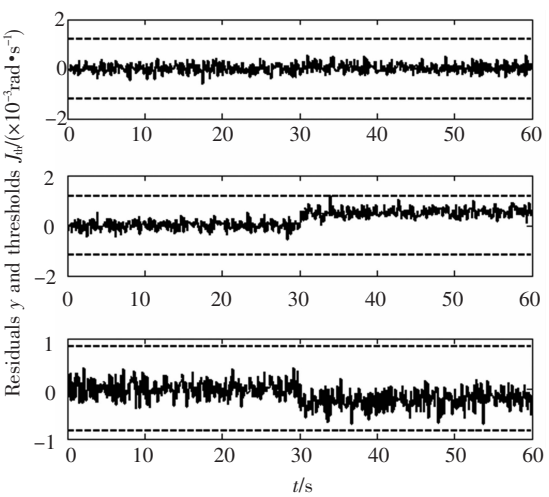

Fig. 10 Residuals and thresholds without filtering

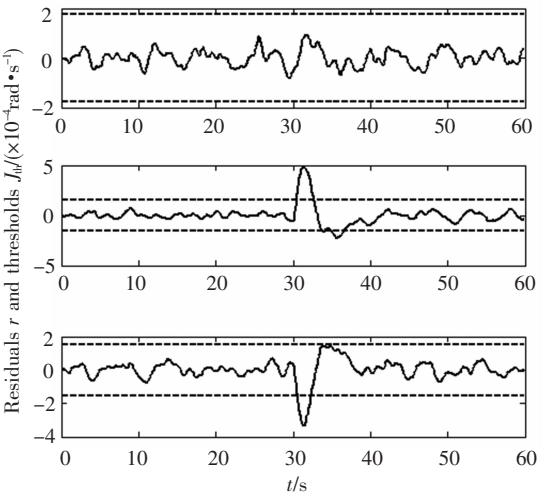

Fig. 11 Residuals and thresholds with filtering

8 Conclusions

A new cascade H_∞ observer design for the Attitude control system of spacecraft is proposed and applied in the gyro and star sensor fault diagnosis problem. This method, which is derived from H_∞ design problem can solve G&S simultaneous fault problem in the condition of existing uncertainties. The use of robust residual for unknown inputs is demonstrated and the CPD controller is applied to ACS. A systematic design procedure that can be carried out using Matlab/Simulink software is presented. Simulation results demonstrate the effectiveness and feasibility of the proposed fault diagnosis and fault-tolerant control algorithm.

References:

[1] Willsky A S. A survey of design methods for failure detection in dynamic systems. IEEE Transactions on Automatic Control, 1976, 12(6): 601 – 611.

[2] Satin A L, Gates R L. Evaluation of parity equations for gyro failure detection and isolation. Journal of Guidance and Control, 1978, 1(1): 14 – 20.

[3] Friedland B. Treatment of bias in recursive filtering. IEEE Transactions on Automatic Control, 1969, 14(4): 359 – 367.

[4] Kim P S. Separate-bias estimates scheme with diversely behaved biases. IEEE Aerospace and Electronic Systems, 2002, 38(1): 333 – 339.

[5] Peyman S, Alireza K, Ebrahim F. Attitude estimates by separate-bias Kaman filter-based data fusion. The Journal of Navigation, 2004, 57(2): 261 – 273.

[6] Frank P M. Fault diagnosis in dynamic systems using analytical and knowledge-based redundancy——A survey and some new results. Automatica, 1990, 26(3): 459 – 474.

[7] Zhong M, Ding S X, Lam J, *et al*. An LMI approach to design robust fault detection filter for uncertain LTI systems. Automatica, 2003, 39(3): 543 – 550.

[8] Chen R H, Mingori D L, Speryer J L. Optimal stochastic

fault detection filter. Automatica, 2003, 39(3): 377 – 390.

[9] Hammouri H, Kinnaret M, Elyaagoubi E H. Observer-based approach to fault detection and isolation for nonlinear systems. IEEE Transactions on Automatic Control, 1999, 44(10): 1879 – 1884.

[10] Kabore P, Wang H. Design of fault diagnosis filters and fault-tolerant control for a class of nonlinear systems. IEEE Transactions on Automatic Control, 2001, 46(11): 1805 – 1810.

[11] Pirmoradi F N, Sassani F, Silva C W. Fault detection and diagnosis in a spacecraft attitude determination system. Acta Astronautica, 2009, 65(5 – 6): 710 – 729.

[12] Kristiansen R, Loria A, Chaillet A, *et al*. Spacecraft relative rotation tracking without angular velocity measurements. Automatica, 2009, 45(3): 750 – 756.

[13] Dalsmo M, Maas W C. Singular H_∞ suboptimal control for a class of nonlinear cascade systems. Automatica, 1998, 34(12): 1531 – 1537.

[14] Frank P M, Ding S X. Survey of robust residual generation and evaluation methods in observer-based fault detection systems. Journal of Process Control, 1997, 7(6): 403 – 424.

[15] Ding S X, Guo L, Frank P M. A Frequency domain approach to fault detection of uncertain dynamic systems. Proceedings of the 32nd IEEE CDC. San Antonio, USA, 1993. 1722 – 1727.

[16] Zhang P, Ye H, Ding S X, *et al*. On the relationship between parity space and H_2 approaches to fault detection. Systems & Control Letters, 2006, 55(2): 94 – 100.

[17] Wertz J R. Spacecraft Attitude Determination and Control. Dordrecht, Holland: Reidel Publishing Company, 1978. 25 – 26.

[18] Zhou K, Doyle J C. Essentials of Robust Control. New York: Prentice-Hall, 1998. 288 – 293.

[19] Pertew A M, Marquez H J, Zhao Q. H_∞ observer design for lipschitz nonlinear systems. IEEE Transactions on Automatic Control, 2006, 51(7): 1211 – 1216.

[20] Song B. Robust Control of Spacecraft Attitude. Harbin: Harbin Institute of Technology, 2007.